

# Inertial Dynamic Effect on the Rates of Diffusion-Controlled Ligand-Receptor Reactions<sup>†</sup>

Woojin Lee,<sup>‡</sup> Ji-Hyun Kim, and Sangyoub Lee\*

Department of Chemistry, Seoul National University, Seoul 151-747, Korea. \*E-mail: sangyoub@smu.ac.kr

<sup>‡</sup>Corporate R&D Institute, Samsung Electro-Mechanics Co. Ltd., Suwon 443-743, Korea

Received March 14, 2011, Accepted April 1, 2011

It has been known that the inertial dynamics has a little effect on the reaction rate in solutions. In this work, however, we find that for diffusion-controlled reactions between a ligand and a receptor on the cell surface there is a noticeable inertial dynamic effect on the reaction rate. We estimate the magnitude of the inertial dynamic effect by comparing the approximate analytic results obtained with and without the inertial dynamic effect included. The magnitude of the inertial dynamic effect depends on the friction coefficient of the ligand as well as on the relative scale of the receptor size to the distance traveled by the ligand during its velocity relaxation time.

**Key Words :** Inertial dynamic effect, Ligand-receptor reactions, Diffusion-controlled reactions

## Introduction

Biochemical processes occurring in a living system are controlled by the recognition of small molecules (called ligands) by the receptors on the cell surface. A proper interpretation of the experimental results on the ligand-receptor interactions requires a detailed analysis of their binding kinetics in solution phase. The rate of binding of a ligand onto its receptor at the cell surface is often diffusion-influenced,<sup>1-3</sup> and various aspects affecting the kinetics have been investigated.<sup>4-10</sup>

In the present work, we investigated the inertial dynamic effect (IDE) on the diffusion-controlled ligand-receptor binding kinetics. The kinetics of diffusion-controlled reactions in solutions has usually been described by the Smoluchowski equation, which neglects the inertial motions of the reactants so that the applicability is limited to the high-friction regime. To take account of the IDE, one needs to consider the Fokker-Planck-Kramers equation but its solution is very difficult to obtain.<sup>11-13</sup> We will therefore introduce a simple reaction model that yields an approximate analytic result.

In a previous work,<sup>14</sup> we estimated the IDE on the reaction between simple hard-sphere reactants by comparing the diffusive Brownian dynamics (BD) simulation results with those obtained from Langevin dynamics (LD) simulation. The diffusion coefficients of the reactants were calculated from separate molecular dynamics (MD) simulations with the solvent molecules modeled also as hard spheres. At the normal liquid densities, the IDE decreases the reaction rate by 19% when the reactants have the same size as the solvent molecules. As expected, the IDE turned out to be smaller when the size of the reactants gets larger than the solvent molecules. When the radius of the reactants is twice of that of solvent molecules, the magnitude of inertial dynamic

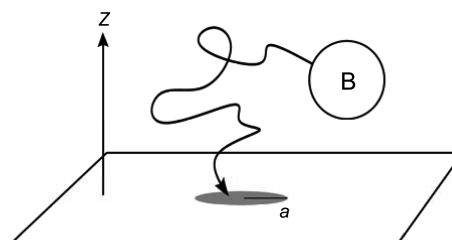


**Figure 1.** A simplified model of ligand-receptor reaction.  $a$  is radius of the reactive patch of the receptor, and B denotes a ligand.

effect reduces to 11%.

It must be noted that the above estimates of the IDE were calculated for the cases where the reactants are spheres with uniform reactivity. The reactant molecules usually have a localized reaction site. Only when the diffusive rotational motion of the reactant occurs rapidly, it can be modeled as a uniformly reacting hard sphere. In many biochemical reactions, one of the reactants is better modeled as a large immobile object with a highly localized reaction site. The binding of a ligand onto the receptor at the cell surface is such an extreme case. It is of interest to estimate the IDE in this case.

We consider a model reaction system depicted in Fig. 1. For simplicity, we model the ligands as spherical Brownian particles that move independently over an infinite plane. The receptor is represented as a circular reactive patch with radius  $a$  on the plane. The reaction is assumed to occur when the ligand approaches the reactive patch within a preset distance. We compare the steady-state reaction rate constants calculated with and without the IDE included. It turns out that the IDE on the ligand-receptor reaction can be quite significant.

## Theory

We consider two types of irreversible reactions that may be schematically represented as  $A+B \rightarrow A+P$  (Type 1) and

<sup>†</sup>This paper is dedicated to Professor Eun Lee on the occasion of his honourable retirement.

$A+B \rightarrow P$  with  $[A] \ll [B]$  (Type 2). In Type 1 reactions, the receptor  $A$  acts as an enzyme that converts the ligand (substrate)  $B$  to a product  $P$ . In Type 2 reactions, the deactivated receptor  $A$  becomes an activated form  $P$  upon capturing the ligand  $B$ . The usual kinetic observables are the survival probabilities  $S_B(t)$  of a ligand molecule for Type 1 reactions, and  $S_A(t)$  of a free receptor for Type 2 reactions.

When the interaction between ligands and their competition for the reaction with the receptor can be neglected, these survival probabilities decay according to

$$S_B(t) = \exp(-[A] \int_0^t d\tau k_f(\tau)) \quad \text{and} \quad S_A(t) = \exp(-[B] \int_0^t d\tau k_r(\tau)) \quad (1)$$

with the time-dependent rate coefficient given by<sup>14,15</sup>

$$k_f(t) = k_R \int d\Lambda S(\Lambda) \rho(\Lambda, t) \quad (2)$$

Here,  $\Lambda$  denotes the set of relevant coordinates describing the reaction progress between  $A$  and  $B$ . If one neglects the IDE,  $\Lambda$  includes only the position vector  $\mathbf{r} [= (r, \theta, z)]$  where  $(r, \theta, z)$  are the cylindrical coordinates with the coordinate origin at the center of the reactive patch in Fig. 1. On the other hand, if the IDE is to be included,  $\Lambda$  should also include the velocity that is conjugated to  $\mathbf{r}$ .

$k_R$  is a constant measuring the intrinsic reactivity and has the dimension of inverse time.  $S(\Lambda)$  is a dimensionless sink function, and  $k_R S(\Lambda)$  represents the rate of disappearance of a ligand due to reaction when its phase space coordinates are given by  $\Lambda$ . Hence the range of  $S(\Lambda)$  defines the reaction zone at which the reaction can occur.

$\rho(\Lambda, t)$  represents the nonequilibrium pair correlation; that is,  $[B] \rho(\Lambda, t) d\Lambda$  gives the number of ligands within the phase-space volume element  $d\Lambda$  at  $\Lambda$  that has survived by time  $t$ . Hence, we have  $\int d\Lambda \rho(\Lambda, t) = V$  with  $V$  denoting the volume of the reaction system.  $\rho(\Lambda, t)$  evolves in time according to the reaction kinetic equation given by<sup>14</sup>

$$\frac{\partial}{\partial t} \rho(\Lambda, t) = [\mathcal{L}(\Lambda) - k_R S(\Lambda)] \rho(\Lambda, t), \quad (3)$$

Here,  $\mathcal{L}$  is the time-evolution operator governing the nonreactive dynamics of a ligand.

We assume that the ligands are distributed in equilibrium at  $t = 0$ ; that is,  $\rho(\Lambda, t=0) = g(\Lambda)$  with  $g(\Lambda)$  denoting the equilibrium pair correlation function. A formal solution to Eq. (2) is then given by

$$\hat{\rho}(\Lambda, s) = [s - \mathcal{L} + k_R S]^{-1} g(\Lambda) = s^{-1} \sum_{n=0}^{\infty} [-[s - \mathcal{L}]^{-1} k_R S]^n g(\Lambda) \quad (4)$$

where the hat denotes the Laplace transform. From Eqs. (1) and (4), we obtain

$$\hat{k}_f(s) = s^{-1} k_R \sum_{n=0}^{\infty} (-1)^n \hat{D}_n(s) k_R^n, \quad (5)$$

where  $\hat{D}_n(s)$  is the Laplace-transformed  $n$ th-order sink-sink correlation function defined by

$$\hat{D}_n(s) = \int d\Lambda S(\Lambda) [(s - \mathcal{L})^{-1} S(\Lambda)]^n g(\Lambda) \quad (6)$$

The [1/1] Padé approximant to the power series in Eq. (5) is given by

$$\hat{k}_f(s) \cong \frac{k_R V_{rx}}{s [1 + k_R \hat{D}_1(s) / V_{rx}]} \quad (7)$$

with  $V_{rx} \equiv \hat{D}_0(s) = \int d\Lambda S(\Lambda) g(\Lambda)$ . This type of rate expression was first obtained by Wilemski and Fixman (WF) by introducing a so-called closure approximation.<sup>16</sup> The key dynamic quantity  $D_1(t)/V_{rx}$  can be roughly interpreted as the returning probability  $P_{ret}(t)$  that a ligand initially located in the reaction zone will be found again in the reaction zone at a later time  $t$  in the absence of reaction. Its more explicit expression is given by

$$D_1(t)/V_{rx} = V_{rx}^{-1} \int d\Lambda S(\Lambda) \int d\Lambda_0 G(\Lambda, t | \Lambda_0) S(\Lambda_0) g(\Lambda_0) \equiv P_{ret}(t), \quad (8)$$

where  $G(\Lambda, t | \Lambda_0)$  is the Green's function defined by

$$G(\Lambda, t | \Lambda_0) = e^{t\mathcal{L}} \delta(\Lambda - \Lambda_0) \quad (9)$$

In the limit of  $k_R \rightarrow \infty$  and  $s \rightarrow 0$ , Eq. (7) gives the steady-state diffusion-controlled reaction rate constant,

$$k_{SS} \cong \frac{V_{rx}}{P_{ret}(0)} \quad (10)$$

Hereafter, we will assume that the potential of mean force between the ligand and the receptor can be neglected. If the inertial effect on the Brownian motion of the ligand cannot be neglected,  $\mathcal{L}$  should be represented by the Fokker-Plank operator,

$$\mathcal{L}(\Lambda) = \mathcal{L}_{FP}(\mathbf{r}, \mathbf{v}) = -\mathbf{v} \cdot \nabla_{\mathbf{r}} + \gamma \nabla_{\mathbf{v}} \cdot \mathbf{v} + \gamma \frac{k_B T}{m} \nabla_{\mathbf{v}}^2 \quad (11)$$

Here  $\gamma$  and  $m$  denote the friction coefficient and the mass of a ligand, respectively. On the other hand, if the inertial effect can be neglected,  $\mathcal{L}$  can be approximated by the diffusion operator,

$$\mathcal{L}(\Lambda) = \mathcal{L}_D(\mathbf{r}) = D \nabla_{\mathbf{r}}^2, \quad (12)$$

with the diffusion coefficient given by the Einstein relation,  $D = k_B T / m \gamma$ .

Since we want to evaluate the inertial effect on the rate of diffusive approach of the ligand, we should use the same reaction model whether the inertial effect can be neglected or not. We thus take a sink function of the form

$$S(\Lambda) = S(\mathbf{r}) = H(a-r) H(z) H(\Delta z - z), \quad (13)$$

where  $H(x)$  is the Heaviside step function and  $\Delta z$  is the thickness of the reaction zone (see Fig.1). If  $\Delta z$  is small enough, Eq. (13) tells that the ligand undergoes reaction when it approaches the reactive patch of radius  $a$  within the distance  $\Delta z$  regardless of its velocity.

When the IDE can be neglected, we take  $\Lambda = \mathbf{r}$  and  $g(\Lambda) = 1$ . The Green's function in Eq. (8) can be obtained by solving  $\partial G / \partial t = \mathcal{L}_D G$  with the reflecting boundary condition

$(\partial G/\partial z)_{z=0} = 0$ . Its explicit expression in the Laplace domain is given by<sup>17</sup>

$$\hat{G}(\mathbf{r}, s | \mathbf{r}_0) = \frac{1}{4\pi D} \int_0^\infty dk \frac{k}{\eta} [e^{-\eta|z-z_0|} + e^{-\eta|z+z_0|}] J_0(kR), \quad (14)$$

where  $\eta = (k^2 + s/D)^{1/2}$ ,  $R^2 = r^2 + r_0^2 - 2rr_0 \cos(\theta - \theta_0)$ , and  $J_\nu(x)$  is the  $\nu$ th-order Bessel function of the first kind.

The steady-state rate constant expression in Eq. (10) can be evaluated with Eqs. (8), (13) and (14) by using the addition theorem for the Bessel function  $J_0(kR)$ ,<sup>18</sup>

$$J_0(kR) = J_0(kr)J_0(kr_0) + 2 \sum_{n=1}^{\infty} J_n(kr)J_n(kr_0) \cos(n(\theta - \theta_0)). \quad (15)$$

We obtain

$$k_{SS}^{BD}(x) = \left( \frac{3\pi^2 Da}{8} \right) \left[ \frac{3\pi}{8x^2} \left( \frac{32}{45\pi} - \frac{3x}{8} - \frac{1}{32x} {}_4F_3 \left( \frac{1}{2}, 1, 1, \frac{5}{2}; 2, 3, 4; -\frac{1}{x^2} \right) + \frac{x}{2} \ln 4x \right) \right] \quad (16)$$

Here,  $x \equiv \Delta z/a$  and  ${}_pF_q(a_1, \dots, a_p; b_1, \dots, b_q; x)$  is the generalized hypergeometric function. The superscript 'BD' means that the result can be verified by the diffusive Brownian dynamics simulations. It is worthy to note that  $k_{SS}^{BD}(x \rightarrow 0) = 3\pi^2 Da/8$  and this limiting expression coincides with that obtained by Shoup, Lipari and Szabo using the constant-flux approximation.<sup>5</sup> This coincidence says that the constant flux approximation is equivalent to the WF approximation at least in the present reaction model with  $\Delta z = 0$ .

To include the IDE, we take  $\Lambda = (\mathbf{r}, \mathbf{v})$  and  $g(\Lambda)$  is given by the Maxwell-Boltzmann velocity distribution  $f_{MB}(\mathbf{v})$ . Then, Eq. (8) reduces to

$$P_{ret}(t) = V_{rx}^{-1} \int d\mathbf{r} S(\mathbf{r}) \int d\mathbf{r}_0 G_I(\mathbf{r}, t | \mathbf{r}_0) S(\mathbf{r}_0), \quad (17)$$

where  $V_{rx} = \int d\mathbf{r} S(\mathbf{r}) = \pi a^2 \Delta z$  and  $G_I(\mathbf{r}, t | \mathbf{r}_0) \equiv \int d\mathbf{v} \int d\mathbf{v}_0 G(\mathbf{r}, \mathbf{v}, t | \mathbf{r}_0, \mathbf{v}_0, \Lambda_0) f_{MB}(\mathbf{v}_0)$ . It can be shown that  $G_I(\mathbf{r}, t | \mathbf{r}_0)$  is a solution of the generalized diffusion equation,<sup>19</sup>

$$\frac{\partial}{\partial t} G_I(\mathbf{r}, t | \mathbf{r}_0) = D(t) \nabla_{\mathbf{r}}^2 G_I(\mathbf{r}, t | \mathbf{r}_0), \quad (18)$$

with the time-dependent diffusion coefficient  $D(t)$  given by

$$D(t) = D[1 - e^{-\gamma t}]. \quad (19)$$

To solve Eq. (18), we need the time-domain expression for Eq. (14). The inverse Laplace transformation of Eq. (14) gives

$$G(\mathbf{r}, t | \mathbf{r}_0) = \frac{1}{2\pi\sqrt{4\pi Dt}} \left[ e^{-(z-z_0)^2/4Dt} + e^{-(z+z_0)^2/4Dt} \right] \int_0^\infty dk k e^{-k^2 t} J_0(kR). \quad (20)$$

Replacement of  $Dt$  with  $\int_0^t dt' D(t') = D\gamma^{-1}[\gamma t - 1 + e^{-\gamma t}]$  in the right-hand side of Eq. (20) gives the solution of Eq. (18). With the resulting Green's function  $G_I(\mathbf{r}, t | \mathbf{r}_0)$  and the sink function in Eq. (13), the steady-state rate constant expression in Eq. (10) can be evaluated as

$$k_{SS}^{LD}(x) = \left( \frac{3\pi^2 Da}{8} \right) \left\{ \frac{3\pi^{1/2} \gamma}{8cx^2} \int_0^\infty dt A^{1/2} \left[ I_0\left(\frac{1}{2A}\right) + I_1\left(\frac{1}{2A}\right) \right] \left[ e^{-x^2/A} - 1 + \frac{\pi^{1/2} x}{A^{1/2}} \text{erf}(x/A^{1/2}) \right] \right\}, \quad (21)$$

where  $A = c^{-1}[\gamma t - 1 + e^{-\gamma t}]$ ,  $c [= (a^2/D)\gamma^{-1}]$  is the ratio of the diffusion time along the reactive patch to the velocity relaxation time,  $I_\nu(x)$  is the  $\nu$ th-order modified Bessel function of the first kind, and  $\text{erf}(x)$  is the error function. The superscript 'LD' means that the result can be verified by the full Langevin dynamics simulations with the inertial dynamics included.

## Computer Simulations

To evaluate the accuracy of the analytic results, we also calculated the steady state rate ( $k_s$ ) for the reaction between a Brownian particle and a patch on a plane from computer simulations. We employed the simulation protocols developed by our group to calculate the diffusion-controlled reaction rates.<sup>14,20-22</sup>

Each trajectory was started at a random position (and in the case of LD with a random velocity selected from the Maxwell-Boltzmann velocity distribution  $f_{MB}(\mathbf{v})$ ) in the reaction zone. The trajectory was then propagated by using the appropriate move algorithms; we used the Ermak-McCammon method<sup>23</sup> for diffusive BD trajectories and the Ermak-Buckholz method<sup>24</sup> for LD trajectories. We used the variable time steps; the details can be found in Refs. 21 and 22.

When the ligand B moved into the forbidden region ( $z < 0$ ; see Fig. 1), we put it back to the free space just by changing the sign of its  $z$ -coordinate for BD trajectories. For LD trajectories, we changed the sign of the  $z$ -component velocity as well as that of the  $z$ -coordinate. We compared the results of this implementation of collision events between the ligand B and the cell surface with those obtained by using the more sophisticated methods employed in the previous studies<sup>21,22</sup> and found that the results are statistically equivalent.

Trajectories were terminated when their time length exceeded a cutoff time,  $T_{\max}$ . From the record of  $N$  trajectories of time length  $T_{\max}$ , the returning probability  $P_{ret}(t)$  defined by Eq. (8) can be calculated as

$$P_{ret}(t) = \frac{1}{N} (\text{number of trajectories found in the reaction zone at time } t) \quad (22)$$

The steady-state diffusion-controlled reaction rate constant  $k_{SS}$  is determined by  $\hat{P}_{ret}(0)$ ; see Eq. (10). The error in the calculated value of  $\hat{P}_{ret}(0)$  due to the truncation of the trajectories at a finite time  $T_{\max}$  can be corrected by noting the asymptotic behavior of the returning probability;  $P_{ret}(t) \sim P_{ret}(T_{\max}) (t/T_{\max})^{-3/2}$ . We thus have

$$\hat{P}_{ret}(0) = \int_0^\infty dt P_{ret}(t) = \int_0^{T_{\max}} dt P_{ret}(t) + 2P_{ret}(T_{\max})T_{\max} \quad (23)$$

With  $V_{rx} = \pi a^2 \Delta z$ , we can then calculate the rate constant  $k_{SS}$  for the model system from Eq. (10).

In the present work, as the units of mass and length we use the mass  $m$  and the diameter  $\sigma$  of the ligand, respectively. The unit of energy is  $k_B T$ , so that the time unit is  $(m/k_B T)^{1/2} \sigma$ . We carried out simulations for 7 different patch sizes ( $a = 0.1, 0.2, 0.3, 0.4, 0.6, 0.8, \text{ and } 1.0$ ). For each patch size,  $\Delta z$

was varied as 0.01, 0.02, 0.03, and 0.04. The diffusion coefficient were varied as  $D = 0.01, 0.05,$  and  $0.10$ ; the friction coefficient used for LD simulation was then given by  $1/D$ . Most of the BD and LD trajectories were terminated at  $T_{max} = 100$ .

## Results and Discussion

In the diffusive regime, an exact expression for  $k_{SS}^{BD}(x = 0)$  was derived by Hill:<sup>4</sup>

$$k_{SS}^{BD}(x = 0) = 4Da \quad (24)$$

On the other hand, our rate expression in Eq. (16) based on the WF approximation gives

$$k_{SS}^{BD}(x \rightarrow 0) = 3\pi^2 Da/8 \cong 3.7Da, \quad (25)$$

which underestimates the exact value by 7.5%. Our BD simulation method for calculating the diffusion-controlled rate coefficient can be applied to a reaction system involving a sink function with finite width ( $x = \Delta z/a > 0$ ), but the value of  $k_{SS}^{BD}(x = 0)$  can be obtained by extrapolation as displayed in Fig. 2. In the figure, the BD simulation results for  $x > 0$  are represented by the filled squares, which are fitted nicely by the solid curve given by Eq. (16). For comparison, we also draw two horizontal lines representing the two values for  $k_{SS}^{BD}(x = 0)$  given by Eqs. (24) and (25). Since our BD method is also based on the WF approximation, it would give the same error as Eq. (16) in the  $x \rightarrow 0$  limit.

For the LD case, there is no exact result even in the  $x \rightarrow 0$  limit. Hence, we compare the survival probability calculated from our simulation method with that obtained from the direct simulation method. In the direct method, we set up a cubic box of size  $L^3$ , and the reactive patch (see Fig. 1) is located at the center of the bottom face,  $z = 0$ . Then many  $B$  particles are placed randomly in the box. The  $B$  particles do not interact with each other and react independently with the patch. That is, once a  $B$  particle touches the patch, it is removed from the box. We impose the periodic boundary condition in the  $x, y$ -direction. For the  $z$ -direction, we impose a reflecting boundary at  $z = L$  to avoid the unreactive loss of

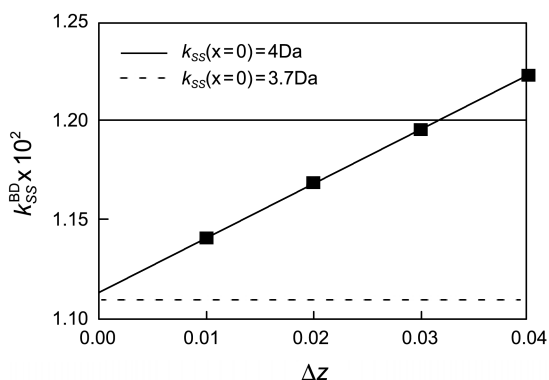


**Figure 2.** Determining the value of  $k_{SS}^{BD}(x = \Delta z/a = 0)$  by extrapolation when  $D = 0.01$  and  $a = 0.3$ .

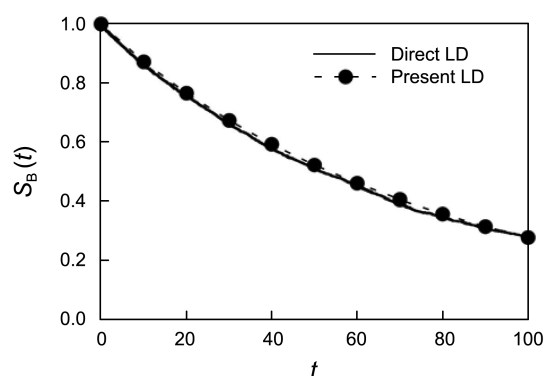


**Figure 3.** Comparison of the direct LD and the present LD results for the survival probability when  $D = 0.1, a = 0.3,$  and  $\Delta z = 0.01$ .

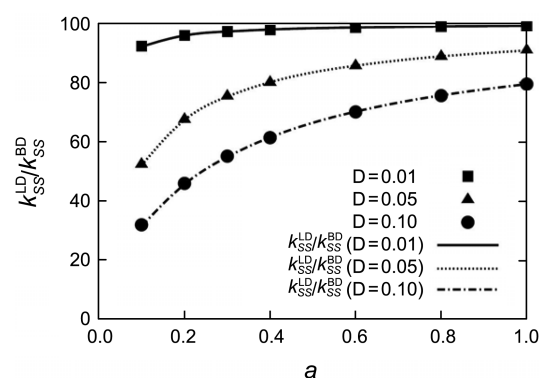


**Figure 4.** The inertial effects on the reaction rate coefficient calculated for  $\Delta z = 0.01$ . Filled squares, triangles, and circles are the results of computer simulations. The solid, dotted, and dot-dashed curves are the results calculated from the analytic expressions given by Eqs. (16) and (21).

the  $B$  particles from the simulation box. The time-dependent survival probability of  $B$  particles calculated directly in this way with  $L = 20$  can be compared with that given by the first expression in Eq. (1). A typical result is shown in Fig. 3. One can see that our LD simulation result, based on the WF approximation, is in good agreement with that obtained from the direct simulation method.

By comparing the BD and the LD results, we can now evaluate the inertial effect on the reaction rate. The result is displayed in Fig. 4. As known from previous studies, the inertial effect retards the reaction rate, and the deviation of the ratio  $k_{SS}^{LD}/k_{SS}^{BD}$  from unity measures the magnitude of the inertial effect. As expected, the inertial effect becomes larger as the friction coefficient,  $k_B T/D$ , gets smaller. An important new finding is that the inertial effect can be quite pronounced when the size of the reactive patch is small. More precisely, it is the ratio of the velocity relaxation time to the diffusion time along the reactive patch that determines the magnitude of the inertial effect, as can be seen from Eq. (21). Equation (21) was derived using the generalized diffusion equation, Eq. (18), in addition to the WF approximation. Nevertheless, as shown in Fig. 4, it provides an accurate estimate for the inertial dynamic effect on the diffusion-controlled, model ligand-receptor reactions.

**Acknowledgments.** This work was supported by the grants from National Research Foundation (NRF), funded by the Korean Government (Grant Nos. 2009-0074693 and 2010-0001631).

### References

1. DeLisi, C. *Q. Rev. Biophys.* **1980**, *13*, 201.
  2. Berg, O. G.; von Hippel, P. H. *Ann. Rev. Biophys. Chem.* **1985**, *14*, 131.
  3. Wiegel, F. W. *Phys. Rep.* **1983**, *95*, 283.
  4. Hill, T. L. *Proc. Nat. Acad. Sci. U.S.A.* **1975**, *72*, 4918.
  5. Shoup, D.; Lipari, G.; Szabo, A. *Biophys. J.* **1981**, *36*, 697.
  6. Keizer, J.; Ramirez, J.; Peacock-Lopez, E. *Biophys. J.* **1985**, *47*, 79.
  7. Baldo, M.; Grassi, A.; Raudino, A. *Phys. Rev. A* **1989**, *40*, 1017.
  8. Barzykin, A. V.; Shushin, A. I. *Biophys. J.* **2001**, *80*, 2062.
  9. Batsilas, L.; Berezhkovskii, A. M.; Shvartsman, S. Y. *Biophys. J.* **2003**, *85*, 1.
  10. Moreira, A. G.; Marques, C. M. *J. Chem. Phys.* **2004**, *120*, 6229.
  11. (a) Harris, S. *J. Chem. Phys.* **1981**, *75*, 3103. (b) Harris, S. *J. Chem. Phys.* **1982**, *77*, 934. (c) Harris, S. *J. Chem. Phys.* **1983**, *78*, 4698.
  12. (a) Naqvi, K. R.; Mork, K. J.; Waldenström, S. *Phys. Rev. Lett.* **1982**, *49*, 304. (b) Naqvi, K. R.; Waldenström, S.; Mork, K. *J. Chem. Phys.* **1983**, *78*, 2710.
  13. (a) Ibuki, K.; Ueno, M. *J. Chem. Phys.* **1997**, *106*, 10113. (b) Ibuki, K.; Ueno, M. *Bull. Chem. Soc. Jpn.* **1997**, *70*, 543.
  14. Lee, J.; Yang, S.; Kim, J.; Lee, S. *J. Chem. Phys.* **2004**, *120*, 7564.
  15. Lee, S.; Karplus, M. *J. Chem. Phys.* **1987**, *86*, 1883.
  16. Wilemski, G.; Fixman, M. *J. Chem. Phys.* **1973**, *58*, 4009.
  17. Carslaw, H. S.; Jaeger, J. C. *Conduction of Heat in Solids*, 2nd ed.; Clarendon Press: Oxford, 1959.
  18. Wang, Z. X.; Guo, D. R. *Special Functions*; World Scientific: Singapore, 1989.
  19. Risken, H. *The Fokker-Planck Equation*, 2nd ed.; Springer: Berlin, 1989.
  20. Lee, S.; Karplus, M. *J. Chem. Phys.* **1987**, *86*, 1904.
  21. Yang, S.; Kim, J.; Lee, S. *J. Chem. Phys.* **1999**, *111*, 10119.
  22. Yang, S.; Han, H.; Lee, S. *J. Phys. Chem. B* **2001**, *105*, 6017.
  23. Ermak, D. L.; McCammon, J. A. *J. Chem. Phys.* **1978**, *69*, 1352.
  24. Ermak, D. L.; Buckholz, H. *J. Comput. Phys.* **1980**, *35*, 169.
-